

RADIATIVE ASPECTS OF TURBULENT PREMIXED COMBUSTION IN LONG FLAME GAS FIRED FURNACES

A. Habibi¹, B. Merci², G. J. Heynderickx³

¹Universite Catholique De Louvain – UCL, Dept. Material and Process, IMAP, Louvain-L.N., Belgium

²Ghent University - UGent, Dept. of Flow, Heat and Combustion Mechanics, Ghent, Belgium

³Ghent University - UGent, Laboratory for Petrochemical Engineering, Ghent, Belgium

MODELING APPROACH

A 3-D RANS simulation of lean premixed turbulent combustion in the firebox of an industrial scale steam cracking furnace is performed. The compressible formulation of RANS equations closed with the Renormalization Group (RNG) $k - \varepsilon$ model¹ along with the standard wall functions² are used. The detail of the modeling is presented elsewhere³. Chemistry is modeled by the C₁ skeletal scheme of Correa⁴. Chemical reactions taking place in turbulent flow are strongly influenced by the turbulent characteristics and the turbulence-combustion interaction. Premixed combustion is viewed as a thin, propagating flame that is stretched and contorted by turbulence. The effect of turbulence is to wrinkle and stretch the propagating laminar flame sheet, increasing the sheet area and, in turn, the effective flame speed. The eddy-dissipation-concept (EDC) model is considered to account for the turbulence-combustion interaction⁵. The system is modeled as a Perfectly Stirred Reactor (PSR) exchanging mass and energy with the surrounding inert fluid. Reactions proceed over the time scale τ^* and the source term in the species transport equation for the mean species i , is modeled as:

$$R_i = \frac{\rho(\xi^*)^2}{\tau^* [1 - (\xi^*)^3]} (Y_i^* - Y_i) \quad (1)$$

where Y_i^* is the fine-scale species mass fraction after reacting over the time τ^* . For steady simulations using the segregated solver, the stiff chemistry solver approximates the reaction rate R_i as:

$$R_i^* = \frac{1}{\tau_i} \int_0^{\tau_i} R_i dt \quad (2)$$

where τ_i is a time-step for integration. The governing combustion equations are stiff and computationally expensive. An In-situ tabulation technique (ISAT)⁶ is used to accelerate the chemistry calculations, offering substantial reductions in run-times. Since radiation is the most significant mode of heat transfer to the tube coils in the furnace, it is critical that the radiation field is accurately represented. The Radiative Transfer Equation (RTE) at position \vec{r} in direction \vec{s} is given by Modest⁷:

$$\frac{dI(\vec{r}, \vec{s})}{ds} + \kappa I(\vec{r}, \vec{s}) = \kappa n^2 \frac{\sigma T^4}{\pi}. \quad (3)$$

Four radiation models are considered: the Rosseland or *diffusion approximation* model⁸, the P-1 model⁹, Discrete transfer⁷ and the Discrete ordinate models¹⁰. The Weighted-Sum-of-Gray-Gases Model (WSGGM) is used to compute the absorption coefficient of the gas mixtures⁷. In this method the nongray gas is replaced by a number of gray gases. Then the total heat flux is found by adding the heat fluxes of the gray gases after multiplication with given weight factors.

SIMULATION DETAIL

A representative segment of an industrial steam cracking furnace is simulated. The segment contains two flame burners that are positioned on the left and the right side of six reactor tubes. Fuel (94.3%

CH₄ and 5.7% H₂ by weight) and air are premixed before entering the firebox. A tetrahedral/hybrid structured meshing scheme is used. The details of imposed boundary conditions and solution procedure are illustrated elsewhere³. The internal emissivity at the burner inlets and outlets is set equal to one. The external black body temperature for the burner inlet and furnace exit is set to 343 K and 1500 K respectively. For DTRM, the ray paths are calculated and stored prior to flow calculations. At each radiating face, rays are traced at discrete values of the azimuthal and polar angles. The number of rays emerging from each cell surface is 64 (4 divisions in θ direction and 16 divisions in ϕ direction). For each iteration, a few numbers of sweeps are performed, until an error tolerance is met or the maximum number of sweeps is reached. The maximum number is set to 10 and the error tolerance is defined as $E = (\sum (I_{new} - I_{old}) / (N\sigma T^4 / \pi)) < 10^{-4}$. E is the summation of the normalized variations in surface intensities from one DTRM sweep to the next. The summation is performed over all radiating surfaces and normalized with respect to the maximum surface emissive power. N is the total number of radiating surfaces. Further increase of the number of sweeps (up to 20) and decrease of the tolerance criterion value (to 10^{-5}) did not show any significant effect on the results. For DOM, each octant of the angular space 4π at any spatial location is discretized into $(N_\theta = 8) \times (N_\phi = 8)$ solid angles. Therefore, a total of $8 \times 8 \times 8$ directions are solved. Since control volume faces do not in general align with the global angular discretization, each overhanging control angle¹¹ is divided into 3×3 pixels.

RESULTS AND DISCUSSION

The turbulent regime is identified as a “thin flame regime with pockets” or “corrugated flamelet regime”. This is characterized by torn flamelets that can be non-contiguous, *i.e.*, a thick turbulent reaction zone containing "islands" of reactants and products in which the reactant pockets are strained by the flow while the reaction front moves into their periphery. Figure 1 shows the temperature contours for each radiation model in the vertical cross section of the furnace at Y=0.6 m through the center of the burners. A clear flame structure is obtained with the P-1 and DOM radiation models.

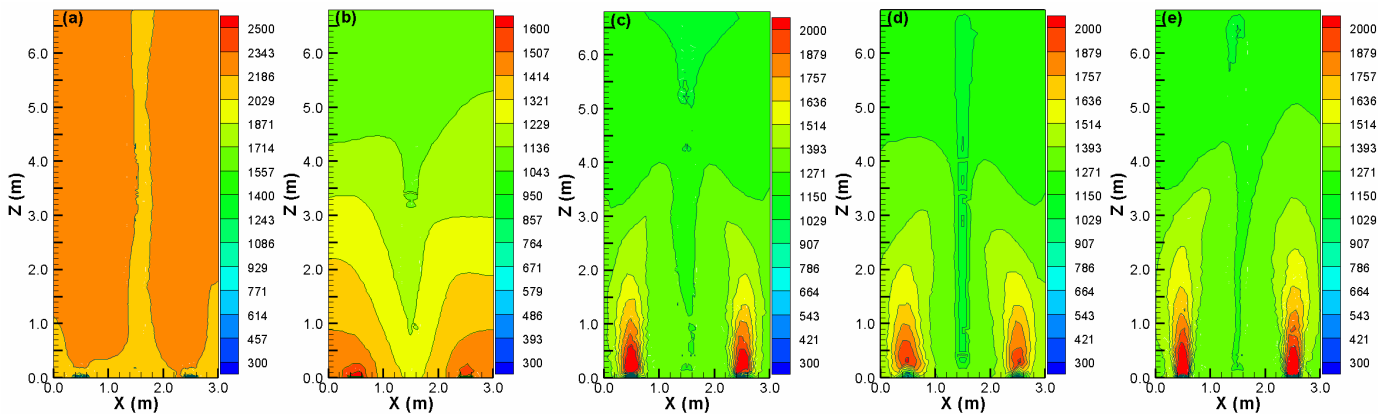


Figure 1: Temperature contours at Y=0.6 m; (a) Adiabatic, (b) Rosseland, (c) P-1, (d) DTRM, (e) DOM.

The predicted temperature field in the adiabatic simulation is clearly unrealistic and the calculated temperatures are too high, due to the absence of radiative heat transfer. With the Rosseland model the effect of radiation is limited to a variation of the radiation conductivity in the energy equation. The temperatures predicted by this model are lower than those predicted by other radiation models. Since in this model the radiation intensity is not obtained from a distinct transport equation, the model cannot precisely predict the flame structure. In Figure 2, the vertical temperature profiles for different radiation

models along the centerline of the left hand side burner are shown. The predictions of DOM and P-1 model are close to each other. The maximum predicted values are occurred around $Z = 0.5$ m. The temperature profiles show that the combustion takes place near the burners and all radiation models show a sharp temperature overshoot close to the burner. The temperature profile the for adiabatic model increases monotonically up to $Z=0.5$ m and flattens asymptotically up to the furnace ceiling. Beyond the flame zone ($Z > 0.5$ m), the difference with other radiation models increases considerably. The predicted temperature difference between the fire-side of the coils and process gas temperature inside the cracking tubes is shown Figure 3.

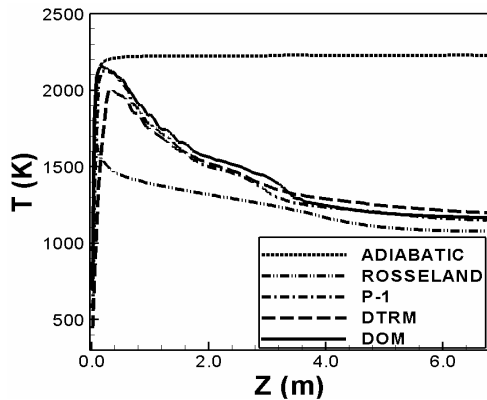


Figure 2: Evolution of the gas temperature at $Y=0.6$ m above the left hand burner.

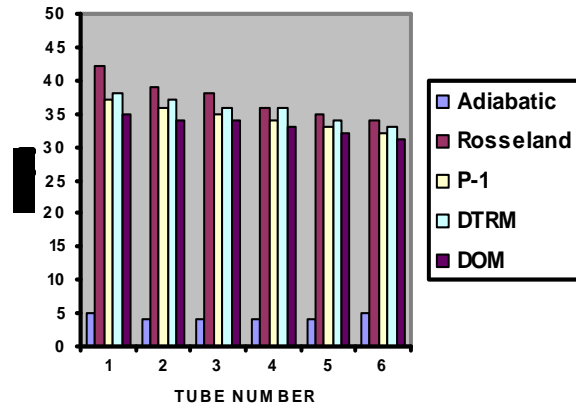


Figure 3: Predicted temperature difference along the cracking tube coils.

It can be seen that except for the adiabatic model, the predicted tube skin temperatures with all radiation models are of the same order. For all radiation models, the predicted temperature increases gradually from the first tube toward the sixth tube. The predicted patterns with various radiation models are realistic, since from the inlet to the outlet of cracking coil, the temperature driving force gradually decreases and consequently a decreasing trend in heat flux along the tubes is observed.

ACKNOWLEDGMENTS

The authors wish to acknowledge the Fund of Scientific Research – Flanders (Belgium) (FWO-Vlaanderen) for financial support through project No. G.0070.03.

REFERENCES

1. Yakhot, V., S. A. Orszag, S. Thangam, T. B. Gatski, C. G. Speziale, *Phys. Fluids A*, **4**, 1510, 1992.
2. Launder B. E., D. B. Spalding, *Computer Methods in Applied Mechanics and Engineering*, **3**, 269, 1974.
3. Habibi A., B. Merci, G. Heynderickx, Submitted to *AICHE J.*, 2007.
4. Correa S. M., *Comb. Flame*, **93**(1-2), 41, 1993.
5. Gran, I. R., Magnussen, B. F., *Combust. Sci. Technol.*, **119**, 191, (1996b).
6. Pope S. B., *Combust. Theory Modelling*, **1**, 41, (1997).
7. Modest, M. F., *Radiative Heat Transfer*, 2nd Edition, Academic Press, (2003).
8. Rosseland S., *Theoretical astrophysics*, Oxford Univ. Press, Clarendon, London and New York, (1936).
9. Siegel R., J. R. Howell, *Thermal Radiation Heat Transfer*. Hemisphere Publishing Corporation, Washington D. C., (1992).
10. Adams B. R., P. J. Smith, *Combustion Science and Technology*, **88**, 293, (1993).
11. Murthy, J. Y., S. R. Mathur, *AIAA-98-0860* (1998).